

## DIRECTIONALITY IN SEISMIC INTENSITY MEASURES: A CASE STUDY OF THE STRONG-MOTION DATABASE OF COSTA RICA

D.A. Hidalgo-Leiva<sup>1</sup>, E. Torres<sup>2</sup> & L.A. Pinzón<sup>3,4</sup>

<sup>1</sup> University of Costa Rica, San José, Costa Rica, [diego.hidalgo@ucr.ac.cr](mailto:diego.hidalgo@ucr.ac.cr)

<sup>2</sup> University of Costa Rica, San José, Costa Rica

<sup>3</sup> Scientific and Technological Research Center, Universidad Católica Santa María La Antigua, Panama City, Panama

<sup>4</sup> Sistema Nacional de Investigación, SENACYT, Panama City, Panama

**Abstract:** *This article presents the results of an analysis of the directionality effect in strong motion records from the Costa Rican Database. A preliminary study was conducted, using four identical sensors placed at a site in different orientations, to validate the theoretical composition of signals used to estimate orientation-independent intensity measures (IMs). Ground motion records from two earthquakes, one from a shallow crustal source and the other from a subduction interface source were used for this purpose. As a result, it was found small differences in the maximum spectral values considering all non-redundant angles (RotD100). This result should not affect larger studies, such as ground motion prediction models or seismic hazard studies, since the differences are negligible. In the analysis of the complete database, a dependence of intensity measures on earthquake magnitude and epicentral distance was identified. Records from earthquakes with larger magnitudes showed a lower RotD100 to geometric mean (GM) ratio, as did records from earthquakes with greater epicentral distance. Based on these results, a proposal to estimate RotD100 from GM values was made. This ratio can be useful to transform values from previous seismic hazard studies, such as those used in seismic codes, and to define the maximum expected seismic intensity for design purposes in a more straightforward manner.*

### 1. Introduction

Accelerographs are instruments used to measure strong ground motion, and they typically collect data in three perpendicular components: two horizontal components aligned with north-south and east-west directions (commonly used at free-field stations) and one vertical component. When working with acceleration data, a notable concern arises regarding how to combine these two orthogonal horizontal components effectively. Conventionally, the geometric mean (GM) of the maximum values is utilized for this purpose, mainly because it reduces variability in the equations used to predict ground motion, referred to as Ground Motion Models (GMMs) (Boore *et al.*, 2006).

However, a significant issue arises due to the orientation of the sensors, as they rarely align with the direction of the highest intensity levels during an earthquake. These high-intensity levels often occur at unpredictable orientations. This phenomenon is known as the earthquake directionality effect.

In this context, numerous studies have emphasized the importance of directionality effects in expected seismic actions, concluding that it is essential to improve predictive equations for strong ground motion in probabilistic seismic hazard analysis (PSHA) to incorporate these effects (Boore, 2010a, Bradley and Baker, 2015, Pinzon, Pujades, Hidalgo-Leiva, *et al.*, 2018, Pinzon *et al.*, 2020, Pinzon, Diaz, *et al.*, 2021, Pinzon, Pujades, *et al.*, 2021). Additionally, other studies propose alternative methods for combining maximum intensity measures (IMs) or peak values, such as those based on temporal combinations of the recorded time histories, which can contribute to obtaining more realistic estimates of expected seismic actions with greater physical significance (Pinzon, Pujades, Hidalgo-Leiva, *et al.*, 2018).

This study investigates how the direction of seismic waves affects the intensity of ground motion, first using two earthquakes and a sensor array and then using data from the Costa Rican Strong Motion Database (CRSMD) (Moya-Fernández *et al.*, 2020). The researchers first computed conventional IMs and orientation-independent IMs for the entire CRSMD database and calculated ratios between the two types of IMs. These ratios can be used to develop correction factors for conventional IMs, so that they can be used to predict the intensity of ground motion more accurately in any direction. Finally, the study proposed correction factors for determining the maximum direction IM (RotD100), based on the GM. This model can be used to more accurately predict the direction from which the strongest seismic waves will arrive at a given site.

The study's findings can be used to improve the design of earthquake-resistant structures and reduce the risk of damage and casualties in future earthquakes.

## 2. Directional variability of ground motion IMs and the impact of sensor orientation

It is well known that orientation-independent IMs can be computed from the orthogonal ground motion signals as-recorded (Boore *et al.*, 2006, Boore, 2010a). To validate this concept, an array with four Reftek 147A tri-axial sensors was deployed at one of the active station sites in the strong ground motion network. This station is located on the University of Costa Rica's property in Fraijanes, Alajuela, and is identified as AFRA. The sensors were connected by wires to two Reftek 130A-01 digitizers, with two sensors assigned to each digitizer. Two GPS antennas were also used, one for each digitizer, to synchronize the signals. The sample rate was configured at 200 samples per second.

The orientation of each sensor is shown in Figure 1. The sensors were positioned about 20 cm from each other (measured from the external faces) and fixed to the reinforced concrete slab. To capture ground motions in various orthogonal planes, the sensors were deliberately installed with angular variations ( $\theta$ ) between them. It's crucial to refer to the angular variations indicated in the figure as a reference since the exact alignment may not be guaranteed due to the sensor installation process. However, it's important to emphasize that this does not diminish the validity of the results obtained.

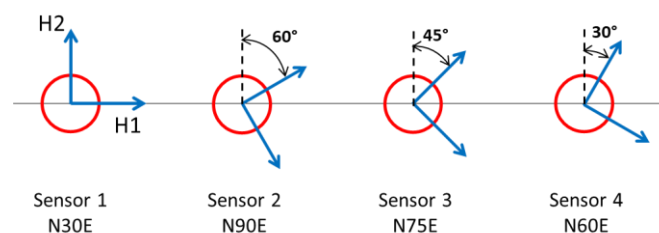


Figure 1. Sensors array orientation. H1 and H2 correspond to the two horizontal sensors' positive orientation. Indicated orientation correspond to H2 azimuth to the magnetic North.

The AFRA station was selected due to the large number of previous records available in the CRSMD and the comprehensive soil characterization of the site. The  $V_{s30}$  value was determined through two MASW lines, resulting in an average value of 333 m/s. Additionally, Pinzon *et al.* (2021) estimate the natural period of vibration of the soil deposit as 0.25 seconds using two different approaches: the ratio of horizontal and vertical spectra from ambient noise and strong motion records. Based on these findings, the site is classified as S2 according to the Costa Rican Seismic Code (CFIA, 2016) and type CD according to ASCE 7-22 (ASCE/SEI, 2022).

The sensor array was active from August 2020 to March 2021, during which it recorded two earthquakes with a PGA greater than 5 cm/s<sup>2</sup>. This threshold was set to ensure an adequate signal-to-noise ratio. The first earthquake, EQ1, occurred on October 24, 2020, at 9:42:08 a.m. local time, with a Moment Magnitude (Mw) of 3.9. Its epicenter was located at a latitude of 9.6080 and a longitude of -83.8830, at a depth of 10 km. The hypocentral distance between the epicenter and the AFRA station was 68.4 km. EQ1 occurred within the Caribbean plate and falls under the Upper Crustal seismic region.

In contrast, the second earthquake, EQ2, occurred on October 31, 2020, at 11:01:09 pm local time, with a magnitude of 5.3 Mw. It had a depth of 74.3 km, and its hypocenter was situated at the interface of the subduction zone, where the Cocos plate subducts beneath the Caribbean plate. This event occurred at a latitude of 9.948 and a longitude of -84.073. The hypocentral distance between the EQ2 epicenter and the AFRA station was 78.3 km.

The vectorial composition of the two horizontal components was used to determine the particle motion in that plane and identify the maximum acceleration ( $acc_{max}$  2D) and its orientation. When the vertical component is included in the vectorial composition, the acceleration orbit can be represented within a sphere, allowing the identification of the maximum acceleration in the space ( $acc_{max}$  3D). These two intensity measures, along with the PGA in H1 and H2 direction, were calculated to compare the results from the recorded earthquakes. Table 1 summarizes the findings.

Table 1. Maximum acceleration and orientation for EQ1 and EQ2.

Event	Sensor	PGA <sub>H1</sub> (cm/s <sup>2</sup> )	PGA <sub>H2</sub> (cm/s <sup>2</sup> )	$acc_{max}$ 2D (cm/s <sup>2</sup> )	Orientation from east (°)	$acc_{max}$ 3D (cm/s <sup>2</sup> )
EQ1	1	5.93	6.29	7.22	240.7	7.27
	2	3.75	6.46	7.24	298.0	7.29
	3	4.34	6.99	7.14	282.0	7.18
	4	5.21	7.09	7.09	269.0	7.12
EQ2	1	10.03	8.92	11.48	29.2	11.48
	2	8.65	11.52	11.54	86.2	11.54
	3	8.23	10.72	11.39	70.2	11.39
	4	8.46	9.51	11.41	56.5	11.41

As anticipated, variations in the maximum acceleration (2D or 3D) fall within the range of 1.32 % to 2.38 % and for most research purposes, these differences can be disregarded. These slight variations are likely attributed to the complex propagation of seismic waves through the ground and the reinforced concrete slab, even though the sensors were affixed close enough to assume a rigid behavior within the slab.

Consequently, it is imperative that the analysis of seismic IMs incorporates the consideration of directionality effects to account for the variations associated with sensor orientation and the direction of seismic wave propagation. This analysis should be extended to include IMs estimated from the acceleration response spectrum (Douglas, 2003, Beyer and Bommer, 2006, Boore *et al.*, 2006, Bradley and Baker, 2015, Boore and Kishida, 2016, Pinzon, Pujades, Hidalgo-Leiva, *et al.*, 2018) given their variation and dependence on the structural natural period of oscillation ( $T_n$ ).

### 3. Directionality effects in the CRSMD

#### 3.1. The CRSMD

The CRSMD 2022 was employed to assess seismic directionality effects on the recorded ground motions. This database encompasses 4,199 digital triaxial records sampled at a rate of 200 Hz, generated from 491 earthquakes. This comprehensive database comprises strong motion time histories and processed data, offering a rich array of intensity measures (as detailed in Moya-Fernández *et al.*, 2020). This database has been used in several studies, including the selection of GMMs for PSHA in Costa Rica, as highlighted in Hidalgo-Leiva *et al.* (2023).

The soil classification within the database was undertaken by Pinzon *et al.* (2021) using Vs30 from MASW tests conducted at 52 stations and the fundamental vibration period of the soil deposits was estimated using the strong ground motions recorded in each station.

### 3.2. Intensity measures

As previously discussed, it's evident that the maximum acceleration and the spectral response of single-degree-of-freedom (SDF) systems have a significant dependency on sensor orientation. This orientation-related variation can also impact the IMs, especially when considering two SDF systems. Figure 2 illustrates this phenomenon, showcasing how the maximum acceleration response (RotD100) of two 5% damped SDF oscillators ( $T_n = 0.20$  s and  $T_n = 1.00$  s) are obtained at different orientations.

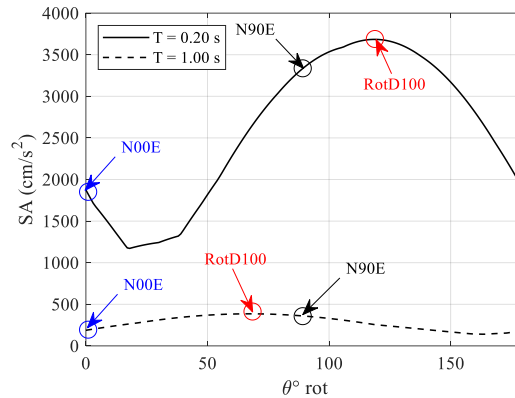


Figure 2. Variation of acceleration response of two 5% damped SDF oscillators ( $T_n = 0.20$  s and  $T_n = 1.00$  s) respect to the sensor orientation from the 5 September 2012 Mw 7.6 Nicoya earthquake recorded at station GNSR.

A MATLAB script, originally developed by Pinzon *et al.* (2018), was adapted to perform a massive calculation involving the two horizontal orthogonal components of the 4,199 selected records. Initially, the 5% damped acceleration response spectra were computed for all the as-recorded signals. This process was then repeated for various linear combinations, considered the rotation angle ( $\theta$ ) variation, spanning from  $1^\circ$  to  $180^\circ$  with increments of  $1^\circ$ . Subsequently, both the sensor orientation-independent and -dependent measures were derived. Table 2 provides a description of the IMs considered in this research. In total, six IMs are considered, where two are dependent on the sensor orientation ( $GM_{ar}$  and Larger), and four are independent ( $GMRotD50$ ,  $GMRotI50$ ,  $RotD50$  and  $RotD100$ ).

Table 2. Considered Intensity measures.

Intensity measure	Definition
$GM_{ar}$	Geometric mean of the response spectra of the two as-recorded horizontal components (Beyer and Bommer, 2006, Bradley and Baker, 2015, Boore and Kishida, 2016, Pinzon, Pujades, Hidalgo-Leiva, <i>et al.</i> , 2018).
Larger	The larger of the two horizontal components (Douglas, 2003, Beyer and Bommer, 2006, Bradley and Baker, 2015, Boore and Kishida, 2016, Pinzon, Pujades, Hidalgo-Leiva, <i>et al.</i> , 2018).
$GMRotD50$	50 <sup>th</sup> percentile of the geometric mean of the response spectra of the two as-recorded horizontal components rotated onto all nonredundant azimuths (Boore <i>et al.</i> , 2006, Boore and Kishida, 2016).
$GMRotI50$	50 <sup>th</sup> percentile of the geometric mean of the response spectra of the two as-recorded horizontal components rotated onto all nonredundant period-independent azimuths (Boore <i>et al.</i> , 2006, Boore and Kishida, 2016).
$RotD50$	50 <sup>th</sup> percentile of the response spectra of the two as-recorded horizontal components rotated onto all nonredundant azimuths (Boore, 2010b, Pinzon, Pujades, Hidalgo-Leiva, <i>et al.</i> , 2018).
$RotD100$	100 <sup>th</sup> percentile of the response spectra of the two as-recorded horizontal components rotated onto all nonredundant azimuths (Boore, 2010b, Pinzon, Pujades, Hidalgo-Leiva, <i>et al.</i> , 2018).

### 3.3. Relationship between different intensity measures and the Geometric Mean of the as-recorded ground motions.

The geometric mean of the response spectra of the as-recorded horizontal ground motion ( $GM_{ar}$ ) has become the predominant definition for the horizontal component in Ground Motion Models (Beyer and Bommer, 2006, Douglas, 2021). Given its wide acceptance and usage, it serves as the reference definition for calculating ratios in this study. These ratios between various IMs enable us to explore variations respect the natural period of SDF systems. These ratios can be applied to convert result from previous studies employing  $GM_{ar}$  as the reference IM, such as earlier PSHA maps.

To estimate the IMs for each record, an extensive analysis of the CRSMD was conducted. Ratios between the IMs introduced in Table 2 and the  $GM_{ar}$  were calculated. These ratios indicate how closely the IMs align with the selected base measure ( $GM_{ar}$ ). If the ratios are close to one, we can infer that the average variation between both IMs is similar, suggesting no significant changes in the current estimated seismic hazard. On the other hand, ratios exceeding one should be considered as an increase in the hazard for that intensity measure in comparison to  $GM_{ar}$ .

Figure 3 illustrates the results after performing the massive analysis. Five mean ratios were obtained and grouped based on maximum and median IMs. In Figure 3a, the mean ratios of maximum spectral values (RotD100 and Larger) to  $GM_{ar}$  are displayed. These ratios range from 1.14 to 1.29. Figure 3b displays the mean ratios between median (50<sup>th</sup> percentile) sensor orientation-independent intensity measures and  $GM_{ar}$  (RotD50/ $GM_{ar}$ ,  $GMRotI50/GM_{ar}$ , and  $GMRotD50/GM_{ar}$ ). Ratios range from 1.01 to 1.04. Lastly, Figure 3c presents the standard deviation of the ratios. To calculate the mean values, the antilogarithm of the average of the natural logarithms of the ratios was used, representing the geometric mean of the ratios (Beyer and Bommer, 2006, Shahi and Baker, 2014). These results are consistent with findings from other regions and databases (Boore *et al.*, 2006, Boore, 2010b, Bradley and Baker, 2015, Pinzon, Pujades, Díaz-Alvarado, *et al.*, 2018, Pinzon, Pujades, Hidalgo-Leiva, *et al.*, 2018, Pinzon, Pujades, *et al.*, 2021).

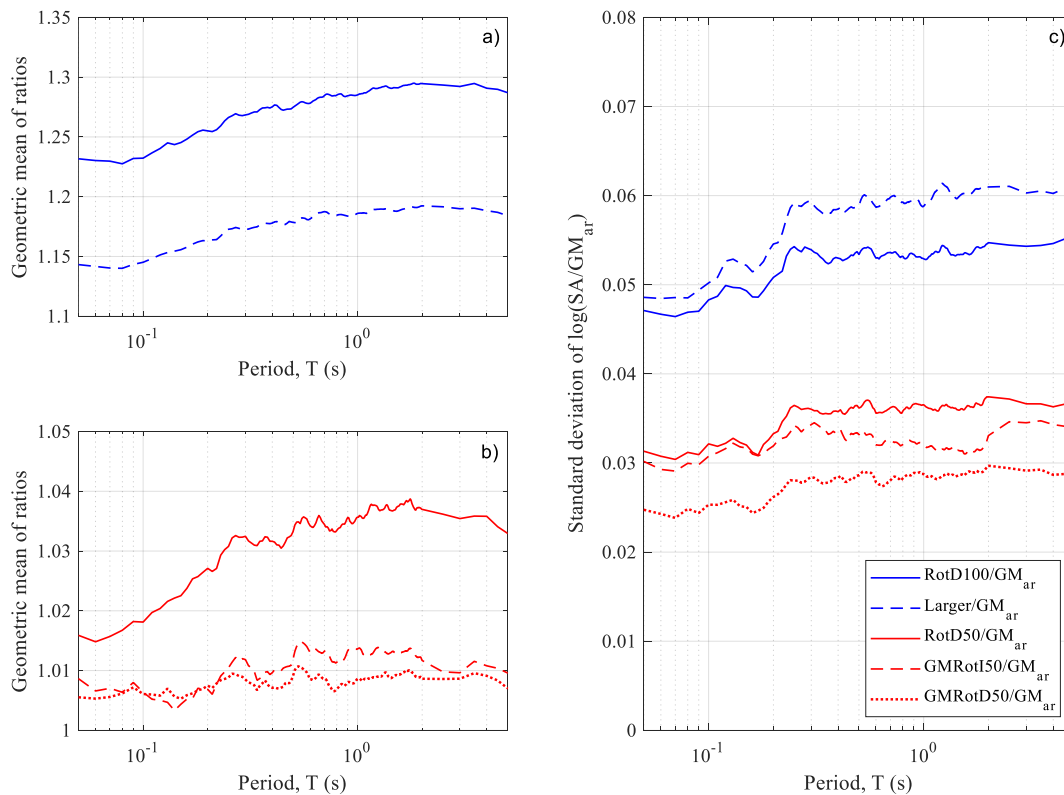
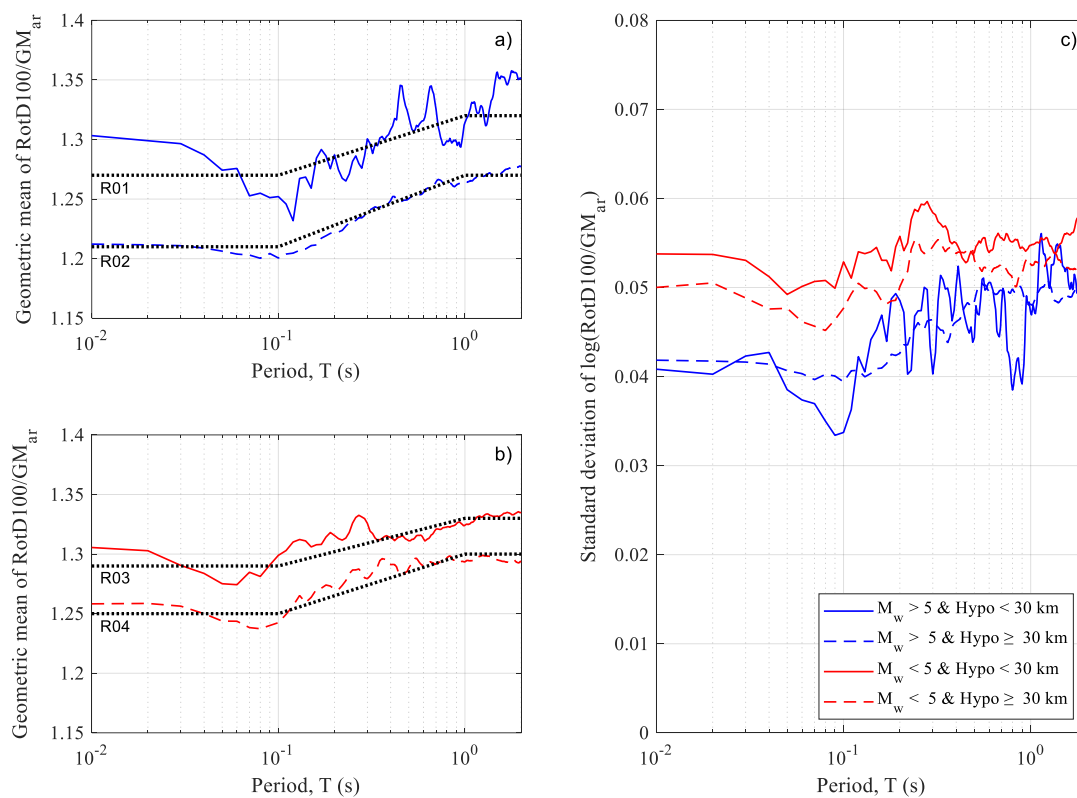


Figure 3. Mean ratios: a)  $RotD100/GM_{ar}$ ,  $Larger/GM_{ar}$  b)  $RotD50/GM_{ar}$ ,  $GMRotI50/GM_{ar}$  and  $GMRotD50/GM_{ar}$ , and c) standard deviation of all ratios

This paper specifically focuses on the maximum direction IM, which can be represented by the RotD100. Some design codes have employed this IM to define the maximum intensity (ASCE/SEI, 2022). Even though the applicability of this measure in design hazard maps has been debated by some authors (Stewart *et al.*, 2011), it is essential to study the variation and dependency on factors like hypocentral distance and earthquake magnitude for a better understanding of this measure. The variation of the RotD100/ $GM_{ar}$  ratio is investigated considering these two independent variables.

Figure 4 displays the results from four sub-databases. Figure 4a, illustrates the variation in ratios for records from earthquakes with a magnitude greater than 5.0  $M_w$ . In the case of near-source record (Hypo < 30 km), the mean ratio increases compared to records from more distant sources. Figure 4b, shows the ratios for earthquakes with a magnitude below 5.0  $M_w$ . Once again, the mean ratios for near-source records are higher than those obtained for records from more distant sources. Finally, Figure 4c has the standard deviation of the presented ratios. The ratios for lower magnitude earthquakes exhibit slightly higher values than those from earthquakes with higher magnitudes; however, these variations are generally negligible.



**Figure 4.** Mean ratios: a) RotD100/ $GM_{ar}$  with  $M_w > 5$  and hypocentral distance greater than or lower than 30km b) RotD100/ $GM_{ar}$  with  $M_w < 5$  and hypocentral distance greater than or lower than 30 km,  $GMRotI50/GM_{ar}$  and  $GMRotD50/GM_{ar}$ , and c) standard deviation of all ratios. The proposed tri-linear models (R01, R02, R03 and R04) are plotted with dotted lines.

Based on these results, a tri-linear model is proposed for these four cases as a simplified representation of the observed mean ratios (dotted lines in Figure 4). This model can be applied as correction factors for a maximum natural period of 2 seconds. The following equations show the proposed model, where R01 corresponds to the scenario of  $M_w > 5$  and Hypo < 30 km, R02 applies to  $M_w > 5$  and Hypo  $\geq$  30 km, R03 is for  $M_w < 5$  and Hypo < 30 km, and R04 is for  $M_w < 5$  and Hypo  $\geq$  30 km:

$$R01 = \begin{cases} 1.27, & T_n < 0.1 \\ 1.27 + 0.05 \left[ \frac{\ln \left( \frac{T_n}{0.1} \right)}{\ln(10)} \right], & 0.1 \leq T_n < 1.0 \\ 1.32, & 1.0 \leq T_n < 2.0 \end{cases} \quad (1)$$

$$R02 = \begin{cases} 1.21, & T_n < 0.1 \\ 1.21 + 0.06 \left[ \frac{\ln \left( \frac{T_n}{0.1} \right)}{\ln(10)} \right], & 0.1 \leq T_n < 1.0 \\ 1.27, & 1.0 \leq T_n < 2.0 \end{cases} \quad (2)$$

$$R03 = \begin{cases} 1.29, & T_n < 0.1 \\ 1.29 + 0.04 \left[ \frac{\ln \left( \frac{T_n}{0.1} \right)}{\ln(10)} \right], & 0.1 \leq T_n < 1.0 \\ 1.33, & 1.0 \leq T_n < 2.0 \end{cases} \quad (3)$$

$$R04 = \begin{cases} 1.25, & T_n < 0.1 \\ 1.25 + 0.05 \left[ \frac{\ln \left( \frac{T_n}{0.1} \right)}{\ln(10)} \right], & 0.1 \leq T_n < 1.0 \\ 1.30, & 1.0 \leq T_n < 2.0 \end{cases} \quad (4)$$

#### 4. Conclusion

This article presents the findings of an evaluation of the directionality effect observed in strong motion records within the Costa Rican Strong-Motion Database. An initial analysis was carried out to validate the theoretical composition of signals used to calculate intensity measures independent of sensor orientation. The results indicate that the variations in Peak Ground Acceleration (PGA) or spectral acceleration with respect to sensor orientation are virtually identical, with variations amounting to less than 2.1% of the maximum. Observed variations were assessed for two distinct earthquakes, and it was observed that these variations are event dependent.

Subsequently, both traditional seismic intensity measures and orientation-independent measures were calculated using the complete strong motion database to establish ratios (referred to as correction factors). This comprehensive analysis encompassed an evaluation of the effects earthquake magnitude, and hypocentral distance have on the ratio that considers the maximum orientation (RotD100) intensity measure.

As a result of this extensive investigation, a model is proposed for determining RotD100 based on the GM, while considering factors such as event magnitude and hypocentral distance. Notably, nearby events, which may be influenced by directivity effects, exhibit the highest values, while distant events with high Moment Magnitude ( $M_w$ ) display the lowest values. This model can be utilized to update GMM or PSHA developed in Costa Rica that were previously based on mean spectral response values.

#### 5. Acknowledgements

This study was supported by the National Secretariat of Science, Technology and Innovation of the Republic of Panama (SENACYT) (grant number FIED 175–2022) and the University of Costa Rica through the project referenced as C2-002 and the National Emergency and Risk Prevention Law N°8488 of the Republic of Costa Rica.

#### 6. References

- ASCE/SEI, (2022). *ASCE/SEI 7-22: Minimum Design Loads and Associated Criteria for Buildings and Other Structures*. Reston, VA: American Society of Civil Engineers.
- Beyer, K. and Bommer, J.J., (2006). Relationships between Median Values and between Aleatory Variabilities for Different Definitions of the Horizontal Component of Motion. *Bulletin of the*

- Seismological Society of America*, 96 (4A): 1512–1522.
- Boore, D.M., (2010a). Orientation-Independent, Nongeometric-Mean Measures of Seismic Intensity from Two Horizontal Components of Motion. *Bulletin of the Seismological Society of America*, 100 (4): 1830–1835.
- Boore, D.M., (2010b). Orientation-Independent, Nongeometric-Mean Measures of Seismic Intensity from Two Horizontal Components of Motion. *Bulletin of the Seismological Society of America*, 100 (4): 1830–1835.
- Boore, D.M. and Kishida, T., (2016). Relations Between Some Horizontal-Component Ground-Motion Intensity Measures Used In Practice 1. *Bulletin of the Seismological Society of America*, 107 (1): 334–343.
- Boore, D.M., Watson-Lamprey, J., and Abrahamson, N.A., (2006). Orientation-Independent Measures of Ground Motion. *Bulletin of the Seismological Society of America*, 96 (4A): 1502–1511.
- Bradley, B.A. and Baker, J.W., (2015). Ground motion directionality in the 2010–2011 Canterbury earthquakes. *Earthquake Engineering and Structural Dynamics*, 44: 371–384.
- CFIA, (2016). *Código Sísmico de Costa Rica 2010 (Revisión 2014)*. 5ta ed. Cartago, Costa Rica: Editorial Tecnológica de Costa Rica.
- Douglas, J., (2003). Earthquake ground motion estimation using strong-motion records: a review of equations for the estimation of peak ground acceleration and response spectral ordinates. *Earth-Science Reviews*, 61 (1–2): 43–104.
- Douglas, J., (2021). *Ground motion prediction equations 1964-2021*. Glasgow.
- Hidalgo-Leiva, D.A., Linkimer, L., Arroyo Hidalgo, I., Arroyo-Solórzano, M., Piedra, R., Climent, Á., Schmidt-Díaz, V., Esquivel, L.C., Alvarado, G.E., Castillo, R., Carranza-Morales, M.E., Cerdas-Guntanis, L., Escalante-Meza, J., Lobo, S., Rodríguez, M.J., and Rojas, W., (2023). The 2022 Seismic Hazard Model for Costa Rica. *Bulletin of the Seismological Society of America*, 113 (1): 23–40.
- Moya-Fernández, A., Pinzon, L.A., Schmidt-Díaz, V., Hidalgo-Leiva, D.A., and Pujades, L.G., (2020). A Strong-Motion Database of Costa Rica: 20 Yr of Digital Records. *Seismological Research Letters*, 91 (6): 3407–3416.
- Pinzon, L.A., Diaz, S.A., Pujades, L.G., and Vargas, Y.F., (2021). An Efficient Method for Considering the Directionality Effect of Earthquakes on Structures. *Journal of Earthquake Engineering*, 25 (9): 1679–1708.
- Pinzon, L.A., Hidalgo-Leiva, D.A., Moya-Fernández, A., Schmidt-Díaz, V., and Pujades, L.G., (2021). Seismic site classification of the Costa Rican Strong-Motion Network based on Vs30 measurements and site fundamental period. *Earth Science Research Journal*, 25 (4): 383–389.
- Pinzon, L.A., Mánica, M.A., Pujades, L.G., and Alva, R.E., (2020). Dynamic soil-structure interaction analyses considering directionality effects. *Soil Dynamics and Earthquake Engineering*, 130 (July 2019).
- Pinzon, L.A., Pujades, L.G., Díaz-Alvarado, S., and Alva, R.E., (2018). Do directionality effects influence expected damage? A case study of the 2017 central Mexico earthquake. *Bulletin of the Seismological Society of America*, 108 (5): 2543–2555.
- Pinzon, L.A., Pujades, L.G., Hidalgo-Leiva, D.A., and Díaz, S.A., (2018). Directionality models from ground motions of Italy. *Ingegneria Sismica*, 35 (3): 43–63.
- Pinzon, L.A., Pujades, L.G., Medranda, I., and Alva, R.E., (2021). Case Study of a Heavily Damaged Building during the 2016 MW 7.8 Ecuador Earthquake: Directionality Effects in Seismic Actions and Damage Assessment. *Geosciences*, 11 (2): 74.
- Shahi, S.K. and Baker, J.W., (2014). NGA-West2 models for ground motion directionality. *Earthquake Spectra*, 30 (3): 1285–1300.
- Stewart, J.P., Abrahamson, N.A., Atkinson, G.M., Baker, J.W., Boore, D.M., Bozorgnia, Y., Campbell, K.W., Comartin, C.D., Idriss, I.M., Lew, M., Mehraian, M., Moehle, J.P., Naeim, F., and Sabol, T. a., (2011). Representation of Bidirectional Ground Motions for Design Spectra in Building Codes. *Earthquake Spectra*, 27 (3): 927–937.